UCID-20336

SIGNAL PROCESSING METHODS FOR MFE PLASMA DIAGNOSTICS

J. V. Candy
T. A. Casper
R. J. Kane

February 1985

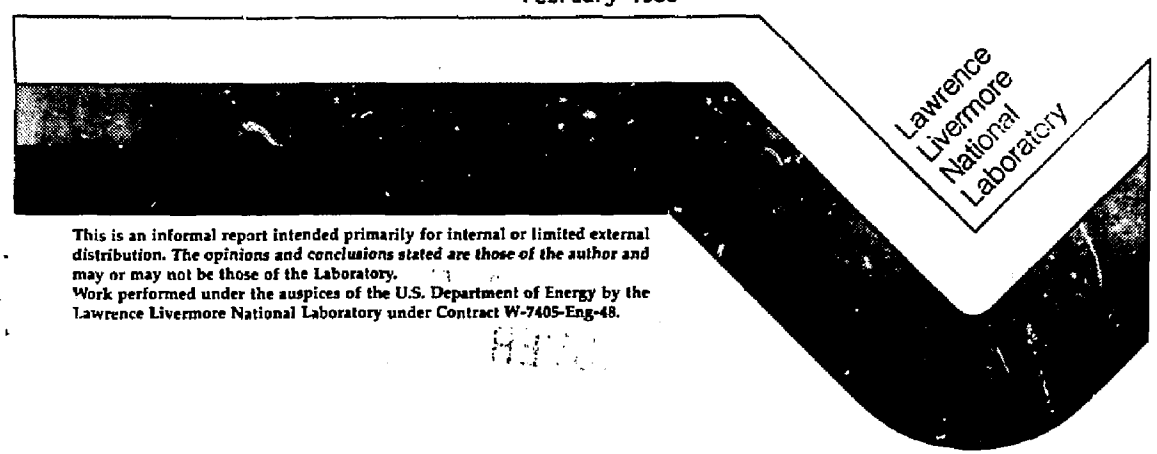

UCID--20336

DE85 007301

Signal Processing Methods for MFE Plasma Diagnostics

J. V. Candy, T. Casper, and R. Kane

CONTENTS

APPENDICES

ABSTRACT

In this report we discuss the application of various signal processing methods to extract energy storage information from plasma diamagnetism sensors occurring during physics experiments on the Tandem Mirror Experiment-Upgrade (TMX-U). We show how these processing techniques can be used to decrease the uncertainty in the corresponding sensor measurements. The algorithms suggested are implemented using SIG, an interactive signal processing package developed at LLNL.

Chapter 1

INTRODUCTION

Controlled *fusion* of heavy isotopes of hydrogen (deuterium and tritium) would enable a virtually limitless supply of energy [1] and therefore provide a solution to the dwindling supply of conventional energy sources. Ultimately, deuterium, which occurs naturally in water, represents a fuel reserve that would last for billions of years. Fusion reactions occur when ions of the hydrogen isotopes, heated to sufficient temperatures, collide and overcome the electrical forces of separation. When the nuclei fuse, enormous amounts of energy are released in the form of neutrons and protons from a relatively small amount of matter. The basic requirement for controlled fusion is to heat a plasma (or ionized gas) to high temperatures, in excess of 10^8 degrees, and confine it for times long enough that a significant number of fusion events occur. In order to confine, heat, sustain, and maintain purity the hot plasma must be isolated in a vacuum from contact with the surrounding vessel walls. One method of accomplishing this is call *magnetic confinement.*

The magnetic confinement method presently used at Lawrence Livermore National Laboratory (LLNL) is the result of over 30 years of research [2,3], starting with a single magnetic mirror cell and evolving to a tandem mirror with thermal barriers [4-6], the Tandem Mirror Experiment - Upgrade (TMX-U) experiment. Results from this experiment are leading to design principles for a commercial reactor. In Figure 1-1 we show a schematic of the TMX-U experiment presently operating at LLNL. As shown in the figure, the tandom mirror consist of a large sausage-shaped region (*central cell*) with a *mirror cell* at each end. Here the magnetic forces confine the plasma within the reacting region until after many collisions they eventually escape. The confining magnetic fields are produced by 24 water cooled coils requiring 20 MW of power to generate peak fields of 2.2T. A target plasma is generated by electrical breakdown of deuterium gas with intense beams of microwaves. The high power microwaves, 800 KW at 24 GHz, also heat the electrons by electron cyclotron resonance heating (ECRH) to temperatures in excess of 50 KeV. Hot deuterium ions are created by ionization and charge exchange with the target plasma of neutral deuterium atoms injected at 15 KeV using a neutral beam system consisting of up to 24 neutral beams producing 5 MW of power for 80 msec pulses. Additional heating of ions can be obtained by ion cyclotron resonance heating (FeRH) using rf power injection of 200 KW in the frequency range of 1.5-4.0 MHz. This electrical environment requires specialized diagnostic sensors and processing techniques to accurately measure plasma parameters without perturbing the confined plasma.

A parameter of significant improtance to magnetically confined plasmas is the diamagnetism of the plasma. This is a measure of the energy density stored in the hot particles. It is also used to determine the beta, β, the ratio of kinetic pressure (nKT) to magnetic field pressure ($B^2/2\mu_0$) and indicates the efficiency of utilization of applied magnetic fields. A single-turn loop transformer is used as the sensor for the plasma diamagnetism [7-9]. As

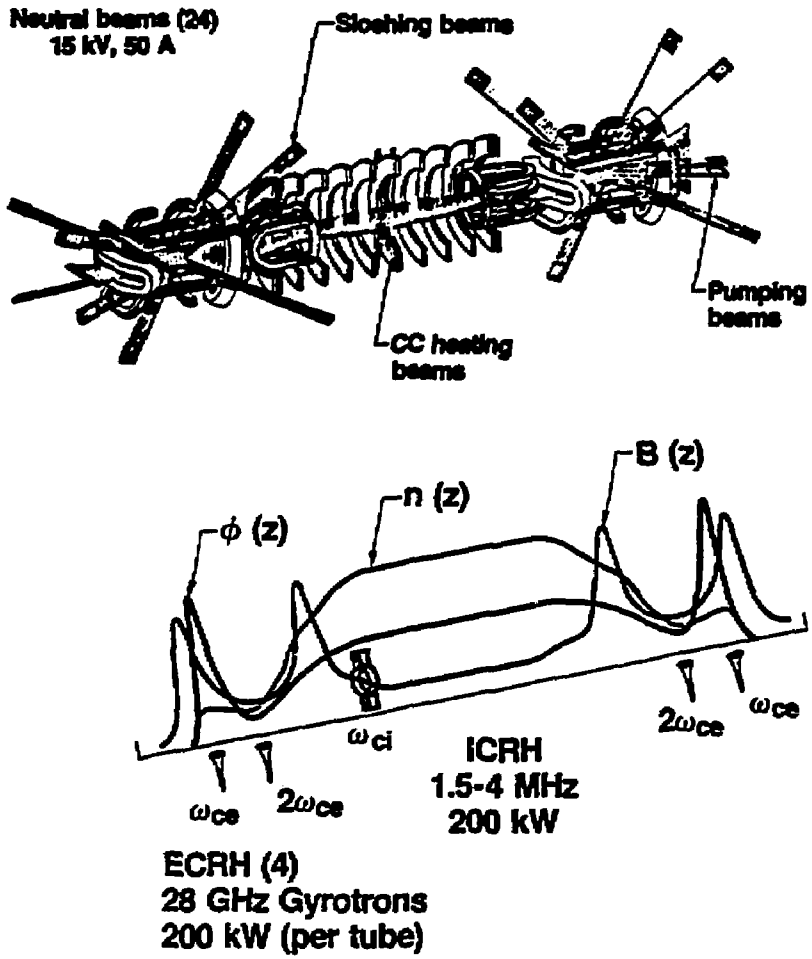

Figure 1-1 Tandom Mirror Experiment-Upgrade (TMX-U)

the plasma particle pressure increases due to heating, it will exclude magnetic field lines from inside thus increasing the apparent magnetic field around the plasm column. The single-turn transformer has $d\phi/dt$ generated as its output. Thus, time integration of this waveform can be used to calculate the plasma, β. On TMX-U we expect values of β up to 0.5 in the end-cell regions.

In the TMX-U plasma, a number of noise sources are present which make the estimation of β difficult. Variations of the magnetic field used to contain the plasma are present because of feedback circuits and ripple currents in the main power system. In many cases the signal that is used to determine the plasma diamagnetism is so badly corrupted with coherent frequency noise (ripple) that the plasma perturbation due to diamagnetism is not even visible. The present noise removal process involves subtraction of a short block of signal that represents the noise component only from data during the time that plasma is present. The noise reference block is aligned in phase with each of the signal plus noise data blocks so that the offending ripple component is removed. The result is integrated and a measure of the plasma diamagnetism is obtained. When the signal are approaching the noise level, or when the feedback control system has introduced a linear trend to the data, this approach is no longer satisfactory. A more sophisticated technique must be used for the processing of the measured signals. It must incorporate trend removal with the capability of removing the coherent noise without affecting the frequency content of the plasma perturbation itself. The development of this technique and associated processing is the goal of this project and discussed in the remainder of this report.

This completes the background information. In the next chapter we discuss the acquisition and processing of the diamagnetic loop measurements for plasma diagnostics. We summarize the results of this effort and present more detailed information about the signal processor employed and the software package (SIG) utilized.

Chapter 2

SIGNAL PROCESSING OF TMX-U MEASUREMENTS

In this section, we analyze the acquired diamagnetic loop (DML) sensor measurements and show how the data can be processed to retain the essential information required for post-experimental analysis. The measured DML data is analog (anti-alias) filtered and digitized at a 25 KHz sampling rate (40 μ sec sample interval). A typical experiment generates a transient signal (plasma) which is recorded for approximately 650 msec (16,384 samples). The raw data and corresponding frequency spectrum are shown in Figure 2-1 along with an expanded section of the transient pulse and noise. We note that the raw data is contaminated with a drift or trend and random noise as well as sinusoidal disturbances at harmonics of 60 Hz, the largest at 360 Hz. The pulse is also contaminated by these disturbances and we see that some of the plasma information appears as high energy spikes(pulses) *riding* on the slower plasma build-up pulse. We will discuss methods to extract this plasma information in a subsequent section, but here we are primarily interested in performing the basic processing to preserve this information and reduce uncertainties in the data.

An examination of the measurement spectrum reveals that most of the plasma information lies below 10 KHz indicating that the data is being slightly oversampled, however. the main objective of sampling in this case is to sample fast enough to preserve the plasma high energy spikes. It is desirable to operate on fewer samples for speed and other numerical reasons, therefore, the raw data was investigated to determine the smallest sampling rate that would preserve the vital plasma characteristics. It was found that the raw DML data could be resampled at a **6.25 KHz** rate (160 μ sec interval) reducing the number of data samples required. The resampled data and spectrum as well as the pulses are show in Figure 2-2. Comparing these results to the previous figure we note very slight differences except in smoothing of the higher frequencies and reduction in noise.

For the purposes of trend and disturbance removal the raw data is partitioned into two sections: one with the disturbances and one with the signal (pulse) and disturbances. These records are then utilized for further processing. The raw processing or pre-processing is automatically accomplished in **SIG**, a software package developed by the Signal and Image Processing Research Group of the Engineering Research Division (EE Department) by selecting the appropriate menu item. The application of SIG to this problem is discussed in Appendix C below.

2.1 *Sinusoidal Disturbance and Trend Removal*

In this section, we discuss the techniques used to enhance and extract the desired signal information from noisy DML measurement data. A close examination of the preprocessed DML data indicates that the data is contaminated by trends, both linear and

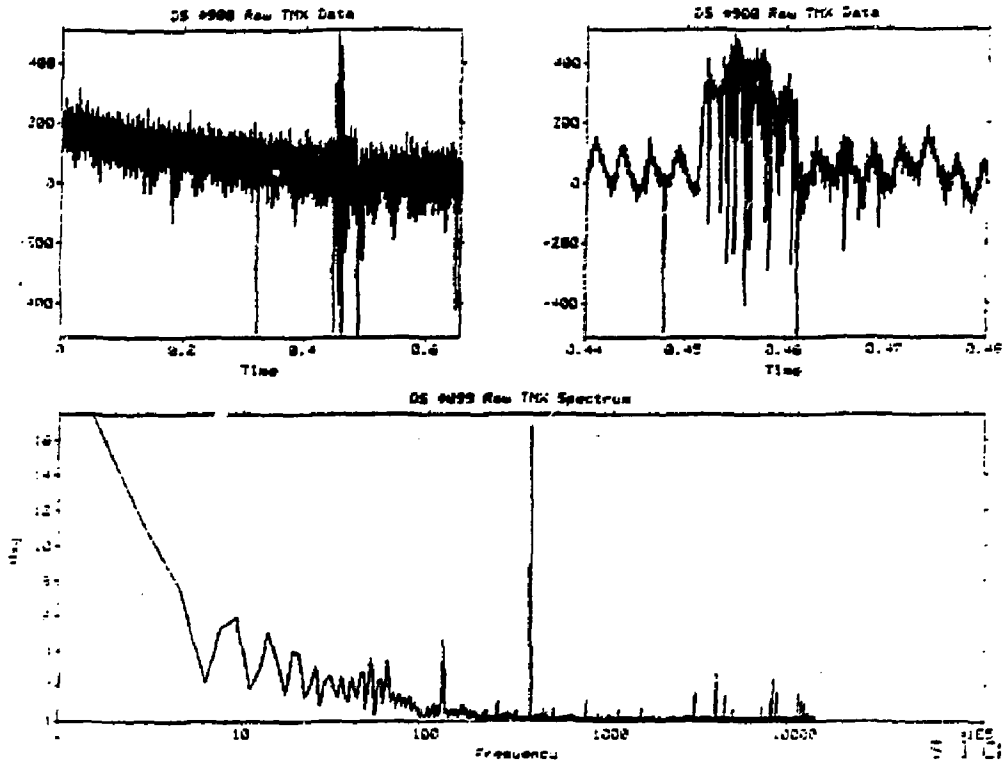

Figure 2-1 Raw Diamagnetic Loop Measurement Data and Spectrum

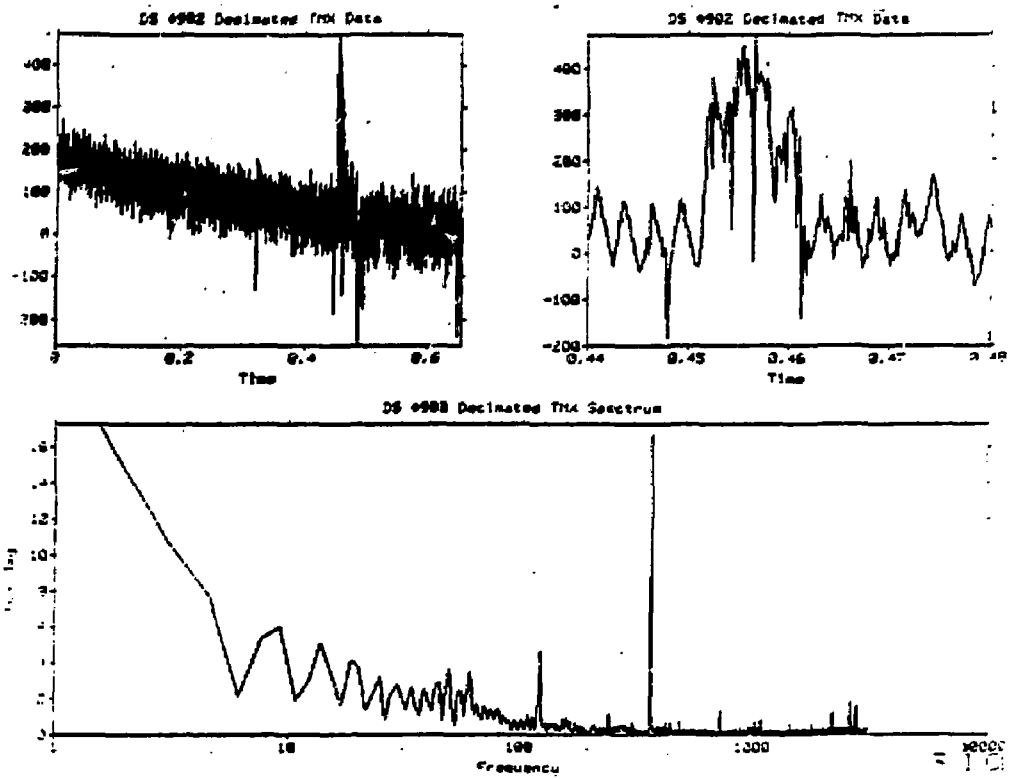

Figure 2-2 Resampled DML Measurement Data and Spectrum

sinusoidal, as well as higher frequency sinusoids and associated harmonics generated by the power supplies utilized in the experiment. The dominant sinusoidal distrubances are at 120 and 360 Hz (see Figure 2-2).

A processor must be developed that will eliminate these disturbances, yet preserve all of the essential features of the transient pulse and associated energy spikes. This problem is ideally suited for a technique called *noise cancelling*. The basic requirements of the data are that a reference file of noise and of the signal and noise are available. For best results, the signal and noise should not be correlated (see *Appendix A* for details). These conditions are satisfied by the DML measurement data, since the onset of the measurement consists only of the disturbances (trend and sinusoids), and the signal is available at the time of the transient pulse. The measured data is modelled by

$$y(t) = s(t) + H(q^{-1})r(t) + v(t) \qquad (2-1)$$

where

y is the measured data,

s is the signal,

H is the sensor or measurement system dynamics,

r is the measured reference noise, and

v is the random disturbance or noise.

The measurement dynamics are given by the polynomial,

$$H(q^{-1}) = h(0) + h(1)q^{-1} + \cdots + h(N)q^{-N},$$

and q is a shift or delay operator (i.e., $q^{-i}r(t) = r(t-i)$).

The noise canceller processes the data and *cancels* the effects of the disturbances by developing an estimate of the system dynamics, $\hat{H}(q^{-1})$, estimating the noise, and then subtracting it from the data to give,

$$z(t) = s(t) + \left[H(q^{-1}) - \hat{H}(q^{-1})\right]r(t) + v(t) \qquad (2-2).$$

Clearly, as $H \rightarrow \hat{H}$, the effects of the disturbances are cancelled. Note that the random or uncorrelated noise, $v(t)$, must still be processed, even after cancelling, since like the signal, it is also uncorrelated with the disturbances.

The noise canceller algorithm was constructed using various commands in **SIG**, and the results are shown in Figure 2-3. Here we see the raw and processed data and corresponding spectra. Note that the sinusoidal disturbances and trend have been eliminated (spectrum) and that the noise spectrum has been reasonably estimated.

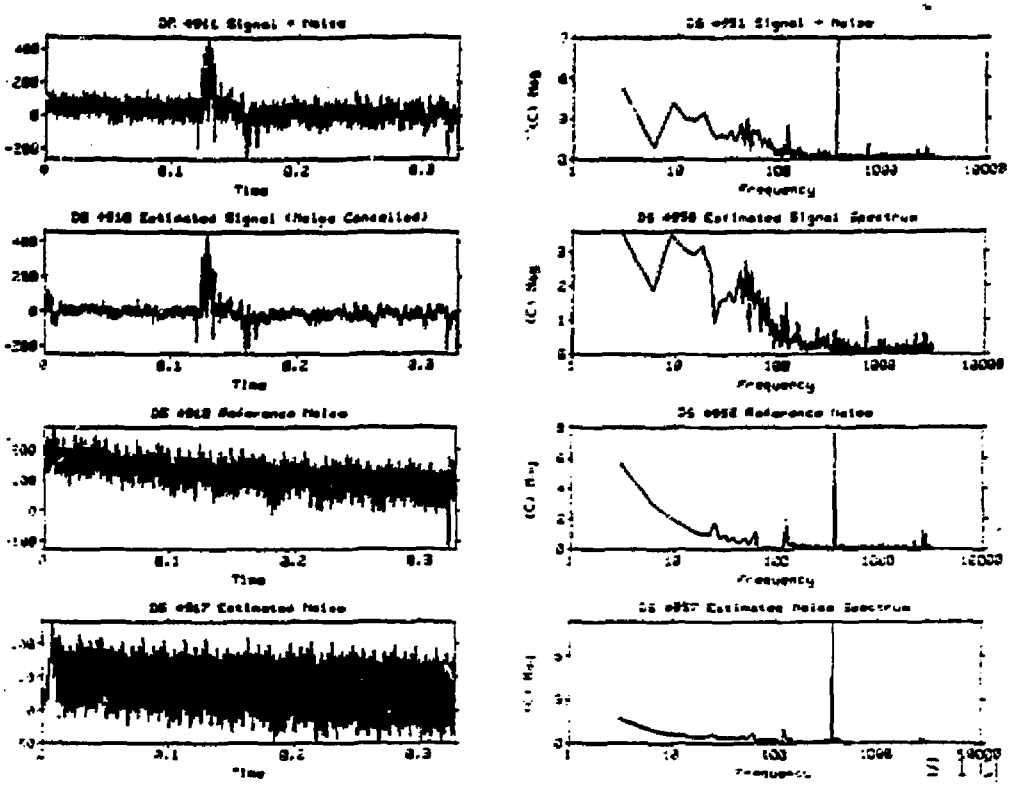

Figure 2-3 DML Disturbanc -noval Using Noise Canceller

A closer examination of the estimated transient pulse (see Figure 2-4) shows that not only have the disturbances been removed, but that the integrity of the pulse has been maintained and all of the high frequency energy spikes have been preserved.

To show the performance of the processor on another independent set of measurements, consider the data show in Figure 2-5. Here we see that the disturbance consists not only of a linear trends but a low frequency sinusoidal trend as well. The raw and processed signal are overlayed for comparative purposes and we see again that the processor is able to reject the disturbances quite well.

Once these disturbances have been removed, the processed signal can be integrated to remove or deconvolve the effects of the differentiating DML probe and provide an estimate of the stored energy build-up in the machine. The results are shown in (see Figure 2-6). The completes the disturbance removal phase of the DML signal processing. In the next section, we show how the TMX-U energy spikes can be extracted from the processed DML data.

2.2 *Energy Spike Estimation*

In this section, we discuss signal processing techniques which can be used to provide estimates of the energy spikes present in the transient plasma build-up. For diagnostic purposes, it is of high interest to be able to extract this information, which previously was not available. One approach to solving this problem is to apply a nonlinear filtering technique called the *median filter*. The noise cancelled data, $\{z(t)\}$, is further processed by selecting a window of a fixed number of samples, sliding it (computationally) through the data, and replacing the current sample value, with the median or middle value (in amplitude) within the window. The effect of this nonlinear operation is primarily to remove the high frequency spikes and provide a *smoothed* estimate of the plasma build-up pulse. Mathematically, this processor can be represented by

$$\hat{x}(t) = Med_{n=0}^{M-1} z(n), \qquad (2-3)$$

where Med $\rightarrow$ means select the median value in the window of length M.

Once the plasma build-up pulse is estimated, it can be subtracted from the cancelled data to provide estimates of the energy spikes of interest, i.e.,

$$e(t) = z(t) - \hat{x}(t). \qquad (2-4)$$

The results of this processing operation is shown in Figure 2-7. First, we see that median filtering the cancelled data, has essentially eliminated all of the high frequency spikes and provided a smoothed estimate of plasma build-up. Next we see the estimated energy spikes. Comparing these estimates to the original data indicates that this procedure gives reasonable estimates. This completes the discussion on signal processing of the DML data, in the next section, we suggest methods that should be investigated to improve the results even further.

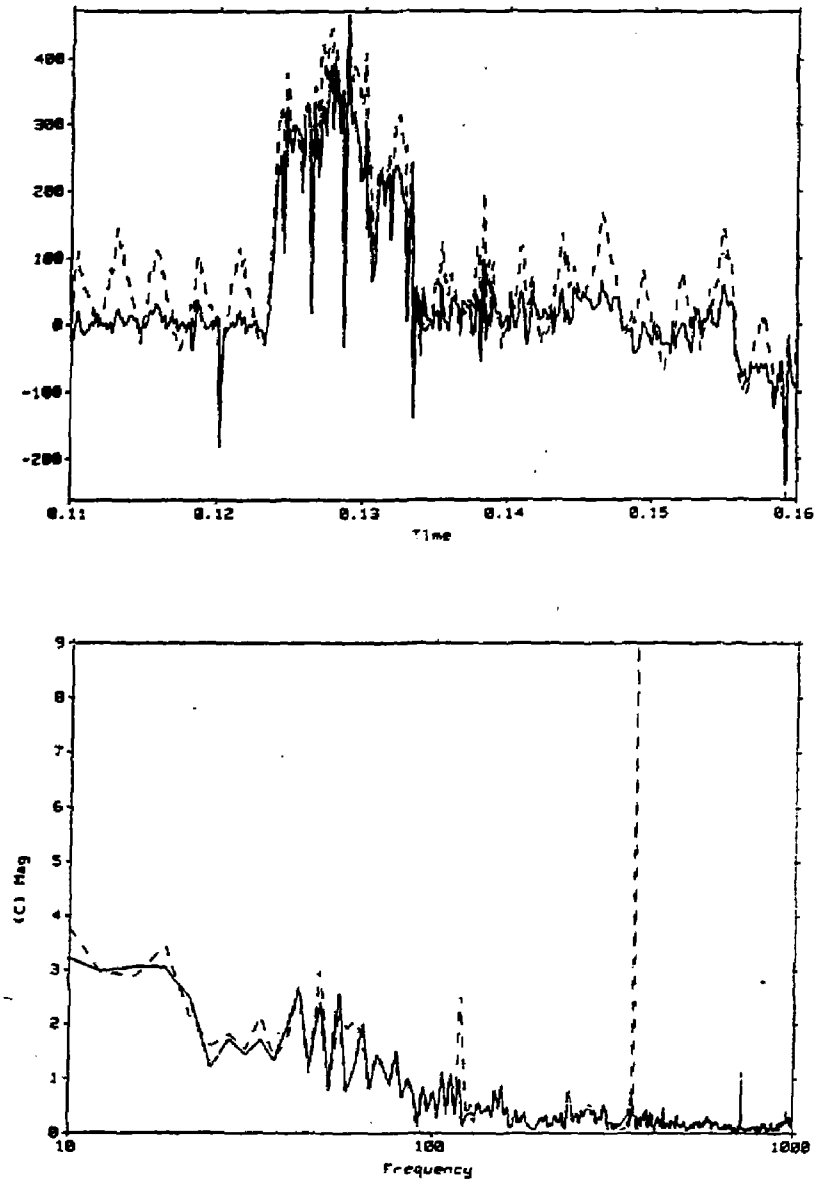

Figure 2-4 Effects of Noise Cancelling on TMX-U Transient Pulse

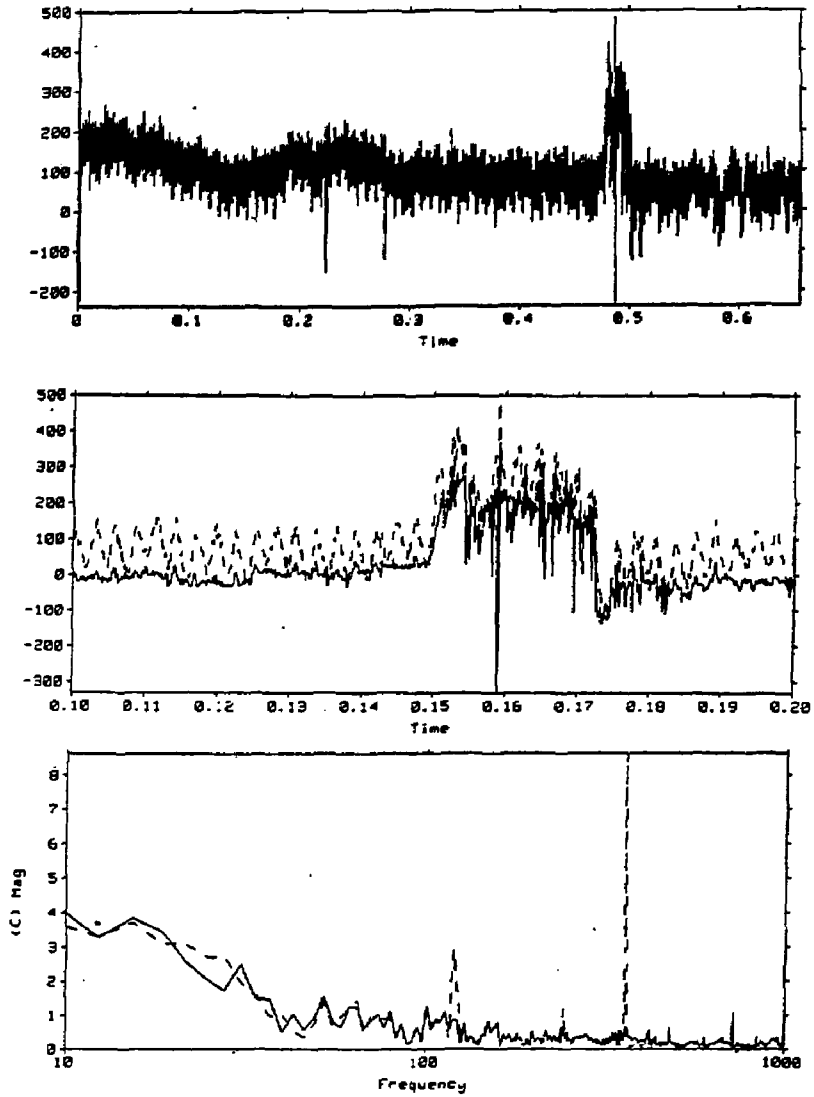

Figure 2-5 Disturbance Removal of Linear and Sinusoidal Trend

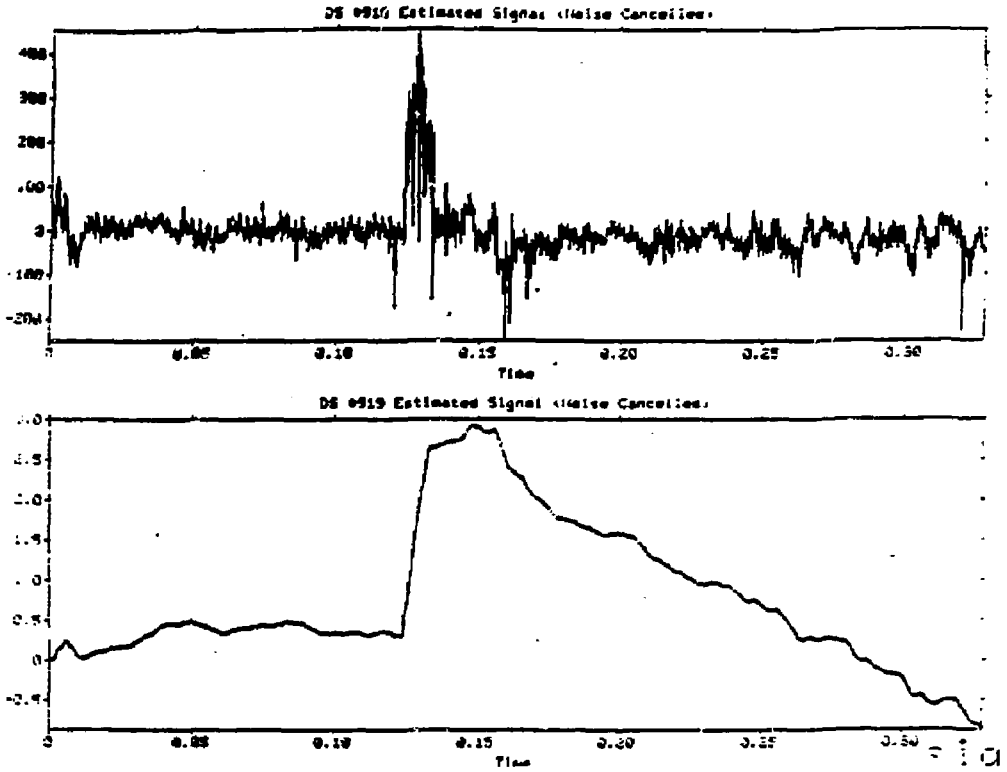

Figure 2-6 Estimated Plasma Build-Up

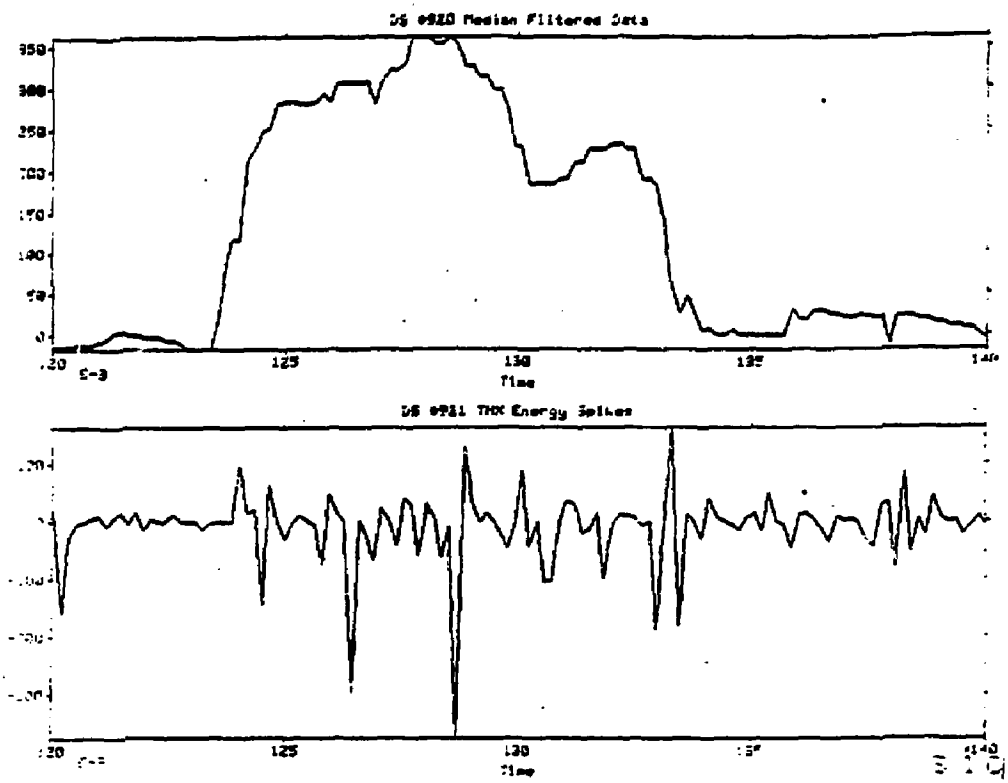

Figure 2-7 Median Filtering and Energy Spike Removal

2.3 *Future Signal Processing*

Various approaches can be taken to process the transient signal resulting from the TMX-U runs. Better estimates of the plasma build-up pulse can be obtained by developing a processor based on the characteristics of the DML, itself. System identification techniques can be applied to independent experimental DML data to obtain a parameterized model of the sensor. Once obtained the model can easily be used to remove the effects of sensor from the acquired data. This approach offers a realistic alternative to merely integrating the cancelled data.

If more specific information about the plasma is required, then one must resort to more powerful model-based signal processing methods to extract it [11]. *Model-based signal processing* is the incorporation of a mathematical model into a processing scheme to extract the desired information. The models primarily describe the underlying phenomenology, in this case the plasma dynamics and characteristics. Processors can easily be constructed which provide more direct information for analysis.

Chapter 3

SUMMARY

In this report, we have discussed the various signal processing methods employed to extract the desired plasma information from measured diamagnetic loop data. We have shown how fundamental signal processing methods can be employed to pre-process the noisy data. The removal of both trends and sinusoidal disturbances was accomplished using noise cancelling signal processing methods. The estimated plasma build-up was provided by integrating the processed data. Next the desired energy spikes were estimated by using a nonlinear filtering method to estimate the plasma build-up pulse and remove it from the data. Finally, we have suggested work for future improvements in signal processing by using model-based methods to extract the information for analysis.

Chapter 4

REFERENCES

[1] The National Mirror Fusion Program Plan, NTIS, UCAR-10042-80, 1980.

[2] Status of Mirror Fusion Research-1980, NTIS, UCAR-10049-80-Rev 1, 1980.

[3] R.Post,"LLL Magnetic Fusion Research: The First 25 Years," **Energy Techn. Rev.**, UCRL-52000-78-5, May, 1978.

[4] TMX Upgrade Major Project Proposal, LLNL-Proposal-172, 1980.

[5] T. Simonen,"TMX Experimental Results," **Energy Techn. Rev.**, UCRL-52000-81-6, June, 1981.

[6] G. Smith,"Understanding Tandem Mirror Devices," **Energy Techn. Rev.**, UCRL-52000-82-11, Nov. 1982.

[7] C. Damm, "The Tandem Mirror MFE Program," **Energy Techn. Rev.**, UCRL-52000-82-8, Aug. 1982.

[8] T. Simonen and G. Leppelmeir,"Diagnostic Instrumentation for Magnetically Confined Plasmas," **Energy Techn. Rev.**, UCRL-52000-79-8, Aug. 1979.

[9] G. Coutts, F. Coffield, and R. Hornady, "Status of Tandem Mirror Experiment-Upgrade (TMX-U) Diagnostic System," **Proc. IEEE Symposium on Fusion Engineering**, and UCRL-89272, 1983.

[10] R. Kane, F. Coffield, G. Coutts, and R. Hornady, "Review of the Tandem Mirror Experiment-Upgrade (TMX-U) Machine-Parameter-Instrumentation System," **Proc. IEEE Symposium on Fusion Engineering**, and UCRL-89264, 1983.

[11] L. Ljung and T. Soderstrom, **Theory and Practice of Recursive Identification**, *M.I.T. Press*:Boston, 1983.

Appendix A

NOISE CANCELLING

In this appendix we derive the algorithm for the noise canceller applied to the plasma diamagnetic signal discussed in Chapter 2 above. The concept of noise cancelling evolves naturally from applications in the biomedical (EKGs, patient monitoring, speech, etc.) and seismological areas (for details see [1]). Ideally, for noise cancelling to be effective the measured data contains little or no signal information for a period of time so that the only information recorded is the noise, therefore, when the signal occurs it is uncorrelated with the reference noise (e.g. pulses in radar, etc.). The initial algorithms developed were adaptive requiring long data records in order for the algorithm to converge (new approaches eliminate this requirement [2]). Variations from the ideal case still met with success. For example, even if signal information is present in the reference record, a reasonable signal estimate can still be obtained. Also, independent measurements can be used rather than the same data record partitioned into reference and signal plus reference. The removal of 60 Hz disturbances can be accomplished by measuring the line voltage as the reference, for instance. In any case, the plasma diagnostics required for monitoring fusion is an ideal candidate for cancelling, since the reference noise can be obtained directly from the measured signal plus noise record and the signal is uncorrelated with the noise.

The fundamental noise cancelling problem is depicted in Figure A-1. Here we assume that the noise corrupting the signal is passed through a linear system,

$$y(t) = s(t) + h_1(t) * n(t) + v_1(t), \qquad (A-1)$$
$$r'(t) = h_2(t) * n(t) + v_2(t) \qquad (A-2)$$

where

y is the measured data

s is the signal

n is the disturbance or noise

v is the random disturbance or noise

r' is the measured reference noise, and

h is the sensor or measurement system dynamics.

The convolution operation * is defined by

$$h(t) * n(t) = \sum_{i=1}^{N} h(i)n(t-i) = \sum_{i=1}^{N} h(i)q^{-i}n(t) = H(q^{-1})n(t)$$

for

$$H(q^{-1}) = h(0) + h(1)q^{-1} + \cdots + h(N)q^{-N},$$

and q is a shift or delay operator (i.e., $q^{-i}n(t) = n(t-i)$).

Thus, using these relations the convolution equations of (A-1,2) can be expressed as

$$y(t) = s(t) + H_1(q^{-1})n(t) + v_1(t), \qquad (A-3)$$
$$r'(t) = H_2(q^{-1})n(t) + v_2(t). \qquad (A-4)$$

The noise cancelling problem can be defined in terms of a parameter estimation problem by eliminating n from the above relations, i.e., if we assume that H_2 is invertible (exists), then we have

$$n(t) = H_2^{-1}(q^{-1})r'(t) - H_2^{-1}(q^{-1})v_2(t).$$

Substituting for n in the measurement equation, we obtain

$$y(t) = s(t) + H_1(q^{-1})\left[H_2^{-1}(q^{-1})r'(t) - H_2^{-1}(q^{-1})v_2(t)\right] + v_1(t),$$

or more simply,

$$y(t) = s(t) + H(q^{-1})r(t) + v(t) \qquad (A-5)$$

where $H(q^{-1}) = H_1(q^{-1})H_2^{-1}(q^{-1})$, $r(t) = r'(t) - v_2(t)$, and $v(t) = v_1(t)$.

Equation (A-5) defines an input/output model for the noise cancelling problem with the input sequence given by $\{r(t)\}$ and the output by $\{y(t)\}$. Using this formulation, we can state the corresponding **noise estimation problem** as

> **Given** the model of (A-5), measurement sequence $\{y(t)\}$, and the noise reference sequence $\{r(t)\}$, **Find** the *best* (minimum error variance) estimate of the noise, n(t).

This problem differs from the classical signal estimation problem† because more information is available about the characteristics of the noise in the reference data. Using the solution to this problem, the canceller is constructed as depicted in Figure A-1. We see at the output of the canceller, that the estimated or filtered response is given by

$$\hat{z}(t) = y(t) - \hat{n}(t). \qquad (A-6)$$

† Actually this estimation problem is a system identification problem as noted by Ljung [3]

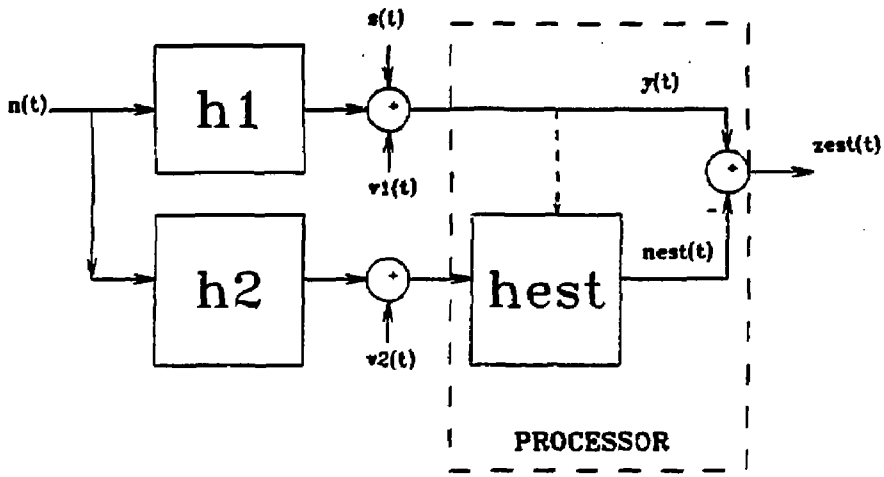

Figure A-1 Noise Cancelling Processor

The minimum variance estimate, $\hat{n}(t)$, removes or cancels the reference noise, as is easily seen by substituting the estimator,

$$\hat{n}(t) = \hat{H}(q^{-1})r(t) \qquad (A-7)$$

above and using (A-5) for $y(t)$ to obtain

$$\hat{z}(t) = s(t) + \left[H(q^{-1}) - \hat{H}(q^{-1})\right]r(t) + v(t). \qquad (A-8)$$

Clearly, as $\hat{H} \rightarrow H$ then $\hat{z} \rightarrow s + v$. If the random measurement noise, $v(t)$ were minimal (small variance), then $\hat{z} \rightarrow s$, i.e., the estimator would provide the minimum variance estimate of s as well, however, for v significant, further processing must be used to obtain the minimum variance estimate of s.

Thus, we see that noise cancelling can be viewed as a two step process:

1. Obtaining the minimum variance estimate of the noise, $n(t)$, and
2. subtracting the estimated noise, $\hat{n}(t)$, from the measured data, $y(t)$.

If we define the criterion function,

$$J(t) = E\{\epsilon^2(t)\}$$

where the error is given by $\epsilon(t) = y(t) - \hat{n}(t)$, then the minimum variance estimator is obtained by finding the $H(q^{-1})$ that minimizes the criterion, i.e.,

$$min_H J(t).$$

The solution to this problem is obtained by differentiating J with respect to each of the $h(i)$, setting the result to zero and solving the resulting set of equations, i.e.,

$$\begin{aligned}\frac{\partial J(t)}{\partial h(k)} &= \frac{\partial}{\partial h(k)} E\{\epsilon^2(t)\} \\ &= 2E\{\epsilon(t)\frac{\partial \epsilon(t)}{\partial h(k)}\}\end{aligned}$$

The error gradient is found by substituting (A-7) for $\hat{n}(t)$ to obtain

$$\frac{\partial \epsilon(t)}{\partial h(k)} = -r(t-k),$$

and therefore,

$$\begin{aligned}\frac{\partial J(t)}{\partial h(k)} &= -2E\{(y(i) + \sum_{i=1}^{N} h(i)r(t-i))r(t-k)\}, \\ &= -2\Big(E\{y(t)r(t-k)\} - \sum_{i=1}^{N} h(i)E\{r(t-i)r(t-k)\}\Big), \quad k = 1, \cdots, N.\end{aligned}$$

Setting this expression to zero and solving, we obtain

$$-R_{yr}(k) = \sum_{i=1}^{N} h(i) R_r(k-i), \quad k = 1, \cdots, N. \qquad (A-9)$$

Carrying out the summations, we obtain the set of linear vector-matrix equations,

$$-\begin{pmatrix} R_{yr}(1) \\ \vdots \\ R_{yr}(N) \end{pmatrix} = \begin{pmatrix} R_r(0) & R_r(-1) & \cdots & R_r(1-N) \\ \vdots & \vdots & \ddots & \vdots \\ R_r(N-1) & R_r(N-2) & \cdots & R_r(0) \end{pmatrix} \begin{pmatrix} h(1) \\ \vdots \\ h(N) \end{pmatrix},$$

or solving for h we obtain

$$\underline{\hat{h}}(N) = -R_r^{-1}(\underline{N}) \underline{R}_{yr}(N) \qquad (A-10)$$

It is straightforward to show that the corresponding error variance, $\hat{R}$, is given by

$$\hat{R} = R_r(0) - \underline{R}'_{ry}(N) R_r^{-1}(\underline{N}) \underline{R}_{yr}(N) \qquad (A-11)$$

This set of linear equations can be solved using standard techniques in linear algebra or since the covariance matrix to be inverted has a Toeplitz structure, a more efficient technique employing the generalized Levinson approach can be applied (see Appendix B for details). Before we close this section, consider the following example to demonstrate the approach.

Example. Suppose we have a simulated pulse disturbed by three sinusoidal signals and zero mean gaussian noise with a standard deviation of 0.01. We apply the noise cancelling algorithm to the contaminated data set, $y(t)$, shown in Figure A-2 along with its corresponding spectrum, $Y(f)$. Note that the pulse spectrum is below 0.01 Hz while the sinusoidal disturbances are at frequencies of 0.01, 0.02, and 0.03 Hz. The output signal-to-noise ratio is high, therefore, the random noise, $v(t)$, is barely noticable. As a reference sequence, we use the noise free sinusoids. The noise canceller is constructed by first calculating the optimal (minimum variance) filter response as in equation (A-10) from estimated correlations, $R_r(k)$ and $R_{yr}(k)$. The estimated response, $\hat{h}(t)$, and corresponding spectrum, $\hat{H}(f)$ are also shown in the figure. Note that the filter is optimized to pass the disturbances (sines and noise) and attenuate any signal information. From the spectrum of $\hat{H}(f)$, we see that the filter will pass frequencies from approximately 0.008 to 0.08 Hz with unity gain and attenuate lower frequencies. Finally, the noise reference sequence, $r(t)$, is filtered (convolved) with $\hat{h}(t)$ to produce the estimated noise, $\hat{n}(t)$ which is then subtracted from the measured data to obtain the cancelled output, $z(t)$. The results of the canceller are also shown in the figure. Note that the desired pulse has been recovered and the sinusoidal disturbances removed or cancelled (see spectra). Also, note that the random noise added to the measured data and not the reference has also been passed by the canceller, since it is also uncorrelated with the reference sequence, as expected. This completes the example.

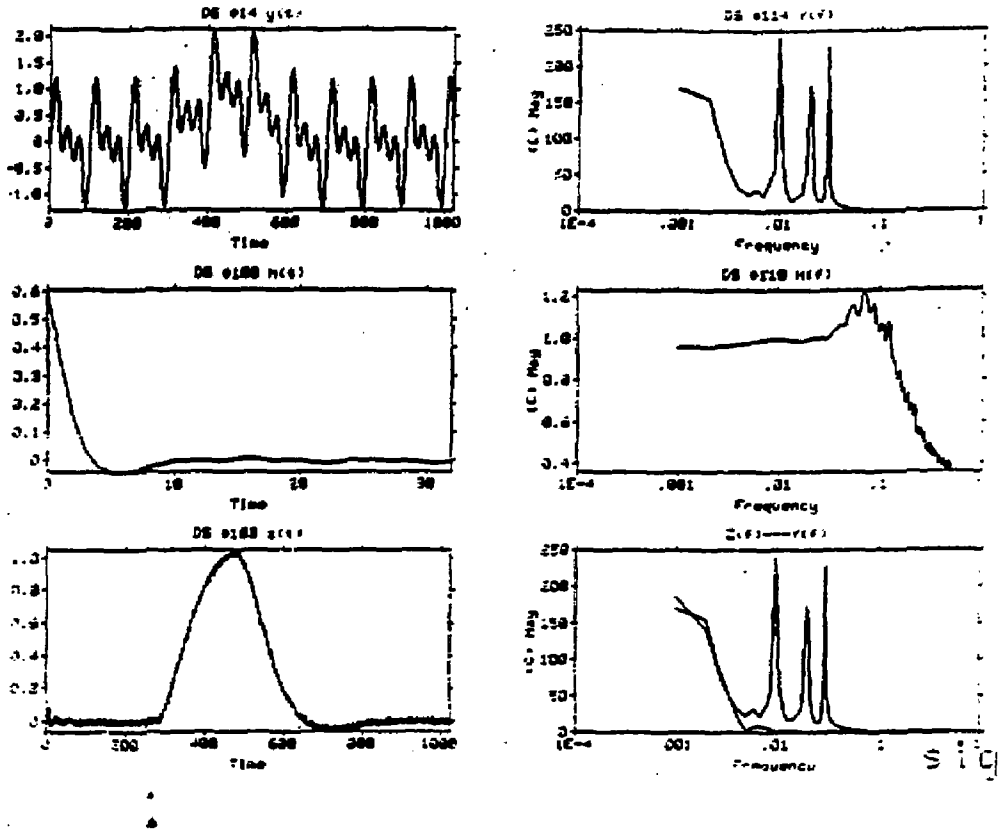

Figure A-2 Noise Cancelling of Sinuosidal Disturbances

So, we see that the noise cancelling concept can be very useful and provide results superior to classical signal estimation when more information is available in a reference sequence.

References

[1] B. Widrow et. al.,"Adaptive noise cancelling: principles and applications," *Proc. IEEE*, vol. 63, 1975.

[2] G. Goodwin and K. Sin, **Adaptive Filtering, Prediction, and Control**, *Prentice-Hall*: New Jersey, 1984.

[3] L. Ljung and T. Soderstrom, **Theory and Practice of Recursive Identification**, *M.I.T. Press*: Boston, 1983.

[4] E. Robinson, **Multichannel Time Series Analysis with Digital Computer Progams**, *Holden-Day*: San Francisco, 1967.

Appendix B

TOEPLITZ INVERSION:

Levinson-Wiggins-Robinson (LWR) Recursion

The noise canceling problem requires the solution of the following set of linear equations

$$\underline{\hat{h}}(N) = -R_r^{-1}(\underline{N})\underline{R}_{yr}(N) \qquad (B-1)$$

where $R_r(\underline{N})$ is a Toeplitz matrix. Efficient algorithms to invert Toeplitz matrices recursively were developed by Levinson [1], and extended to the so-called "generalized" case by Wiggins and Robinson [2]. In this appendix, we develop the **LWR** which is implemented in **SIG** to solve this problem. The **LWR** recursion can be developed in two steps. The first establishes the basic recursion, and the second is the standard Levinson recursion for inverting Toeplitz matrices. We will use the notation $\{h_i^k\}$ to denote the i^{th} coefficient of the k^{th} order filter and the corresponding *autocorrelation* as $r_j = E\{x(t)x(t+j)\}$ and *crosscorrelation* as $g_j = E\{x(t)y(t+j)\}$. In this notation, Eqn. B-1 becomes

$$\underline{\hat{h}}(N) = -R^{-1}(\underline{N})\underline{g}(N) \qquad (B-2)$$

Let us assume that we have the k^{th} order filter that satisfies the set of *normal equations*,

$$\begin{bmatrix} r_0 & \cdots & r_k \\ \vdots & \ddots & \vdots \\ r_k & \cdots & r_0 \end{bmatrix} \begin{bmatrix} h_0^k \\ \vdots \\ h_k^k \end{bmatrix} = -\begin{bmatrix} g_0 \\ \vdots \\ g_k \end{bmatrix} \qquad (B-3)$$

and we want the $(k+1)^{th}$ order solution given by

$$\begin{bmatrix} r_0 & \cdots & r_{k+1} \\ \vdots & \ddots & \vdots \\ r_{k+1} & \cdots & r_0 \end{bmatrix} \begin{bmatrix} h_0^{k+1} \\ \vdots \\ h_{k+1}^{k+1} \end{bmatrix} = -\begin{bmatrix} g_0 \\ \vdots \\ g_{k+1} \end{bmatrix} \qquad (B-4)$$

Suppose the optimum solution for the $(k+1)^{th}$ order filter is is given by the k^{th} order, then $\underline{h}'(k+1) = [\ \underline{h}'(k) \ \vdots\ 0\ ]$ and $\underline{g}'(k+1) = [\ \underline{g}'(k) \ \vdots\ \nabla_k\ ]$ with $\nabla_k = g_{k+1}$. We can rewrite Eqn. B-4 as

$$\begin{bmatrix} r_0 & \cdots & r_k & r_{k+1} \\ \vdots & \ddots & \vdots & \vdots \\ r_k & \cdots & r_0 & r_1 \\ r_{k+1} & \cdots & r_1 & r_0 \end{bmatrix} \begin{bmatrix} \underline{h}(k) \\ \cdots \\ 0 \end{bmatrix} = -\begin{bmatrix} \underline{g}(k) \\ \cdots \\ \nabla_k \end{bmatrix} \qquad (B-5)$$

where $\nabla_i = \sum_{j=0}^{i} h_j^i r_{i-j+1}$.

We must perform operations on Eqn. B-5 to assure that $\nabla_k = g_{k+1}$ for the correct solution. Let us assume there exists a solution $\{\alpha_i^{k+1}\}$ such that

$$\begin{bmatrix} r_0 & \cdots & r_{k+1} \\ \vdots & \ddots & \vdots \\ r_{k+1} & \cdots & r_0 \end{bmatrix} \begin{bmatrix} \alpha_0^{k+1} \\ \vdots \\ \alpha_{k+1}^{k+1} \end{bmatrix} = - \begin{bmatrix} v_{k+1} \\ \vdots \\ 0 \end{bmatrix} \qquad (B-6)$$

Now by elementary manipulations, we can reverse the order of the components, multiply by a constant, K_{k+1} and subtract the result from Eqn. B-5, that is,

$$\begin{bmatrix} r_0 & \cdots & r_{k+1} \\ \vdots & \ddots & \vdots \\ r_{k+1} & \cdots & r_0 \end{bmatrix} \left\{ \begin{bmatrix} h_0^k \\ \vdots \\ h_k^k \\ 0 \end{bmatrix} - K_{k+1} \begin{bmatrix} \alpha_{k+1}^{k+1} \\ \vdots \\ \alpha_1^{k+1} \\ \alpha_0^{k+1} \end{bmatrix} \right\} = - \left\{ \begin{bmatrix} g_0 \\ \vdots \\ g_k \\ \nabla_k \end{bmatrix} - K_{k+1} \begin{bmatrix} 0 \\ \vdots \\ 0 \\ v_{k+1} \end{bmatrix} \right\}$$

or

$$\begin{bmatrix} r_0 & \cdots & r_{k+1} \\ \vdots & \ddots & \vdots \\ r_{k+1} & \cdots & r_0 \end{bmatrix} \left\{ \begin{bmatrix} h_0^k - K_{k+1}\alpha_{k+1}^{k+1} \\ \vdots \\ h_k^k - K_{k+1}\alpha_1^{k+1} \\ -K_{k+1}\alpha_0^{k+1} \end{bmatrix} \right\} = \left\{ - \begin{bmatrix} g_0 \\ \vdots \\ g_k \\ \nabla_k - K_{k+1}v_{k+1} \end{bmatrix} \right\} \qquad (B-7)$$

Here the multiplier K_{k+1} is selected so that

$$\nabla_k - K_{k+1}v_{k+1} = g_{k+1}$$

By identifying the coefficients $\underline{h}(k+1), \underline{g}(k+1)$ from Eqn. B-7 with $\alpha_0^i = 1$, we obtain the first part of the recursion

$$\begin{aligned} &\textit{Initialize}: \quad v_1 = r_0 - r_1^2/r_0, \nabla_0 = r_1 \\ &\textit{For} \quad i = 1, \cdots, k \\ &\nabla_i = \sum_{j=0}^{i} h_j^i r_{i-j+1} \\ &K_{i+1} = \frac{\nabla_i - g_{i+1}}{v_{i+1}} \qquad (B-8) \\ &h_{i+1}^{i+1} = -K_{i+1} \\ &h_j^{i+1} = h_j^i - K_{i+1}\alpha_{i-j+1}^{i+1} \quad \textit{for} \quad 1 \le j \le i \end{aligned}$$

In order to satisfy the recursion, we must obtain, $\{\alpha_i^{k+1}\}, v_{k+1}$ from the solution of Eqn. B-6. Using the same logic as before we assume that $\underline{\alpha}'(k+1) = [\ \underline{\alpha}'(k)\ \vdots\ 0]$ such that

$$\begin{bmatrix} r_0 & \cdots & r_{k+1} \\ \vdots & \ddots & \vdots \\ r_{k+1} & \cdots & r_0 \end{bmatrix} \begin{bmatrix} \alpha_0^k \\ \vdots \\ \alpha_k^k \\ 0 \end{bmatrix} = - \begin{bmatrix} v_k \\ \vdots \\ 0 \\ \Delta_k \end{bmatrix} \qquad (B-9)$$

where the discrepancy $\Delta_i = 0$, if the k^{th} order solution is optimal and Δ_i is given by

$$\Delta_i = \sum_{j=0}^{i} \alpha_j^i r_{i-j+1}$$

Continuing as before, if we reverse the order in Eqn. B-9, multiply by the constant K_{i+1}^*, and subtract, we obtain

$$\begin{bmatrix} r_0 & \cdots & r_{k+1} \\ \vdots & \ddots & \vdots \\ r_{k+1} & \cdots & r_0 \end{bmatrix} \left\{ \begin{bmatrix} \alpha_0^k \\ \alpha_1^k - K_{k+1}^* \alpha_k^k \\ \vdots \\ -K_{k+1}^* \alpha_0^k \end{bmatrix} \right\} = \left\{ - \begin{bmatrix} v_k - K_{k+1}^* \Delta_k \\ 0 \\ \vdots \\ \Delta_k - K_{k+1}^* v_k \end{bmatrix} \right\} \qquad (B-10)$$

where K_{k+1}^* is selected such that

$$\Delta_k - K_{k+1}^* v_k = 0$$

By identifying the coefficients of $\underline{\alpha}(k+1)$, v_{k+1}, we obtain the well-known *Levinson-Durbin* recursion for the $\{\alpha_j^i\}$ as:

$$\begin{aligned} &\textit{Initialize}: \quad v_0 = r_0, \quad \Delta_0 = r_1, \quad K_1^* = -r_1/r_0 \\ &\qquad \textit{For} \quad i = 1, \cdots, k \\ &\qquad \Delta_i = \sum_{j=0}^{i} \alpha_j^i r_{i-j+1} \\ &\qquad K_{i+1}^* = \frac{\Delta_i}{v_i} \qquad (B-11) \\ &\qquad \alpha_{i+1}^{i+1} = -K_{i+1}^* \end{aligned}$$

$$\alpha_j^{i+1} = \alpha_j^i - K_{i+1}^* \alpha_{i-j+1}^i \quad for \;\; 1 \leq j \leq i$$

$$v_{i+1} = v_i - K_{i+1}^* \Delta_i$$

This completes the derivation of the solution to the Toeplitz inversion using the generalized Levinson algorithm.

References

[1] N. Levinson, "A heuristic exposition of Wiener's mathematical theory of prediction and filtering," *J. Math. Phys.*, vol. 25, 1947.

[2] E. Robinson, **Multichannel Time Series Analysis with Digital Computer Progams**, *Holden-Day*: San Francisco, 1967.

[3] E. Robinson and S. Treitel, **Geophysical Signal Analysis** *Prentice-Hall*: New Jersey, 1980.

Appendix C

SIG FOR TMX

In this appendix we discuss the application of **SIG**, a signal processing software package developed by the Signal and Image Processing Group of the EE/Engineering Research Division. **SIG** enables a user to employ various signal processing techniques and develop algorithms by creating command files (in the **SIG** language) and executing them directly or in menu mode. We chose to use the menu mode so that the processing could be automated on the MFE DEC-10 computer system.

The basic **SIG** menu for the TMX diagnostics is shown below in Figure C-1. Here we see that the operations performed are the: (1) pre-processing, (2) plasma build-up estimates, (3) energy spike estimation, and (4) noise cancelling analysis. An example, of a **SIG** command file for the plasma build-up estimates is shown in Figure C-2. Here we see the construction of the cancelling algorithm from **SIG** commands. For example, the noise estimate given by

$$\hat{n}(t) = \hat{h}(t) * r(t),$$

is implemented using the

1. IMPULSE command to estimate, $\hat{h}(t)$, and
2. CONVOLVE command to obtain, $\hat{n}(t)$.

The cancelling algorithm operation is then completed by calculating

$$z(t) = y(t) - \hat{n}(t)$$

using the SUBTRACT command to obtain, $z(t)$.

The cancelled pulse is then integrated (INTEGRATE)to provide an estimate of the plasma build-up phase of the experiment. So, we see how various procedures can be implemented within **SIG** to accomplish the required signal processing tasks for this problem. This completes the appendix on the application of **SIG**.

```
<:::::::::::: MFE: Plasma Diagnostics ::::::::::::>

  1) Pre-process Raw Diagnostic Data

  2) Extract Plasma DML Signal

  3) Extract Plasma Energy Dumps

  4) Exact Noise Canceller

  5) Adaptive Noise Canceller

  6) Analyze Noise Canceller Performance

  7) RETURN to main menu

  8) Exit SIG

Menu item? (0=redisplay, CTRL-Z=return to SIG)>
```

Figure C-1 SIG TMX Diagnostics Menu

```
erase
!_____________________________________________________________________
!||||||||||||||||||||||||||||||||||||||||||||||||||||||||||||||||||||||
!||||||||||||||||||Perform The Basic Signal Processing||||||||||||||||||
!||||||||||||||||||||||||||||||||||||||||||||||||||||||||||||||||||||||
!_____________________________________________________________________
!
!_____________________________________________________________________
!||||||||||||||||||||||||||||||||||||||||||||||||||||||||||||||||||||||
!||||||||||||||||||Remove the Sinusoidal Disturbances||||||||||||||||||
!||||||||||||||||||||||||||||||||||||||||||||||||||||||||||||||||||||||
!_____________________________________________________________________
erase
!_____________________________________________________________________
!||||||||||||||||||||||||||||||||||||||||||||||||||||||||||||||||||||||
!||||||||||||||||||EXACT Noise Canceller||||||||||||||||||||||||||||||
!||||||||||||||||||||||||||||||||||||||||||||||||||||||||||||||||||||||
!_____________________________________________________________________
!
impulse 910 911 915 64 .1          ! Estimate Filter for Noise
dstitle 915 Optimal Impulse Response
convolve 915 910 916               !Estimated Noise
iicut 916 917 1 2048
dstitle 917 Estimated Noise
subtract 911 917 918               !Estimate Signal (Cancelled Noise)
dstitle 918 Estimated Signal (Noise Cancelled)
erase

!_____________________________________________________________________
!||||||||||||||||||||||||||||||||||||||||||||||||||||||||||||||||||||||
!||||||||||||||||||Integrate to Obtain the Energy||||||||||||||||||||||
!||||||||||||||||||||||||||||||||||||||||||||||||||||||||||||||||||||||
!_____________________________________________________________________
integrate 918 919
pfw plot.vpname 2x1
pfw plot.mpmode single
pfw plot.pause page
tsp 918 919
exec restore
```

Figure C-2 SIG Plasma Build-Up Command File